

# Supplementary Information

## Reactive Transport of U and V from Abandoned Uranium Mine Wastes.

*Sumant Avasarala<sup>1</sup>, Peter C. Lichtner<sup>2</sup>, Abdul-Mehdi S. Ali<sup>3</sup>, Ricardo González-Pinzón<sup>1</sup>,  
Johanna M. Blake<sup>4a</sup> and José M. Cerrato<sup>1\*</sup>*

\*Corresponding email address: [jcerrato@unm.edu](mailto:jcerrato@unm.edu)

Telephone: (001) (505) 277-0870

Fax: (001) (505) 277-1918

<sup>1</sup> Department of Civil Engineering, MSC01 1070, University of New Mexico, Albuquerque, New Mexico 87131, USA.

<sup>2</sup> OFM Research-Southwest, Santa Fe, New Mexico 87507, USA.

<sup>3</sup> Department of Earth and Planetary Sciences, MSC03 2040, University of New Mexico, Albuquerque, New Mexico 87131, USA.

<sup>4</sup> Department of Chemistry, MSC03 2060, University of New Mexico, Albuquerque, New Mexico 87131, USA.

<sup>a</sup> Current address: U.S. Geological Survey, New Mexico Water Science Center, 6700 Edith Blvd NE., Albuquerque, New Mexico, USA.

Journal: Environmental Science & Technology

Date: October 5, 2017

28 pages (including cover page)

5 Tables

8 Figures

## Table of Contents

<b>I. Additional Materials and Methods</b> .....	<b>S4</b>
Acid Extractable Procedure.....	S4
Inductively Coupled Plasma (ICP) .....	S4
Transmission Electron Microscope (TEM). .....	S4
Synchrotron Micro- X-ray Fluorescence mapping ( $\mu$ -SXRF).....	S5
Reactive Transport modelling (PFLOTRAN) .....	S5
<b>II. Tables</b> .....	<b>S9</b>
Table S1 .....	S9
Table S2 .....	S15
Table S3 .....	S16
Table S4 .....	S17
Table S5 .....	S18
<b>III. Figures</b> .....	<b>S19</b>
Figure S1 .....	S19
Figure S2.....	S20
Figure S3.....	S21
Figure S4.....	S22
Figure S5.....	S23
Figure S6.....	S24
Figure S7.....	S25
Figure S8.....	S26
<b>IV. References</b> .....	<b>S27</b>

**Additional Materials and Methods.** *Acid Extractable Procedure.* Acid digestions were conducted to assess the total acid extractable metal concentrations between unreacted and reacted mine wastes. For unreacted mine waste 3 mL of hydrochloric acid (HCl), 3 mL of nitric acid (HNO<sub>3</sub>) and 3 mL of hydrofluoric acid (HF) were added into 50 mL Teflon digestion tubes containing  $1 \pm 0.002$  g of mine waste sample. Similarly for reacted mine waste (collected after reaction with CH<sub>3</sub>COOH) 1 mL of each reagent (HCl, HF and HNO<sub>3</sub>) was added to 50 mL Teflon digestion tubes containing  $0.1 \pm 0.002$  g of mine waste sample. All reagents are of Ultra High Purity (UHP) grade. The digestion tubes were then heated using a Digi prep MS SCP Science block digester at 95°C for 2 h, followed by dilution of acid extracts from reacted and unreacted mine waste to 50 (unreacted) and 25 (reacted) mL using 2% HNO<sub>3</sub>. The diluted samples are then filtered using 0.45 µm filters to remove any suspended or undissolved solids before analysis.

*Inductively Coupled Plasma (ICP).* Acid extracts and aliquots from column experiments were analyzed for elemental concentrations using a PerkinElmer Optima 5300DV ICP-OES. Trace metals below the detection limit of ICP-OES were measured using PerkinElmer NexION 300D (Dynamic Reaction Cell) Inductively Coupled Plasma-Mass Spectrometer (ICP-MS). Both ICPs are calibrated with calibration standards and QA/QC measures are taken to ensure quality data.

*Transmission Electron Microscope (TEM).* A TEM analysis was conducted on mine waste samples to identify the crystallinity of various U-V bearing minerals using a Selected Area Electron Diffraction technique (SAED). A JEOL 2010 High Resolution Transmission Electron Microscope (HR-TEM) fitted with a GATAN Orius high speed CCD camera and an Oxford INCA system with an ultra-thin window Energy Dispersive Spectroscopy (EDS) detector was used in sample analysis. Drops of unaltered sediments suspended in acetone were dropped onto

standard holey carbon film-covered Cu TEM grids using a pipette. Acetone was allowed to evaporate in air and then the dry samples were loaded onto a Gatan cryotransfer holder to observe frozen hydrated specimens for cryo-electron microscopy. Before loading the grid, zeolite crystals inside the cryotransfer holders were allowed to dry overnight using a vacuum pump to avoid cooling obstruction due to frozen water inside the holder. The dry and loaded cryotransfer holders were then loaded into the HR-TEM and allowed to reach a temperature of -180°C using liquid nitrogen before the analysis. The INCA EDS detector was used to determine the elemental composition of the specific targeted crystal. After identification, SAED analysis was performed on the identified crystals to observe their crystallinity.

*Synchrotron Micro- X-ray Fluorescence mapping ( $\mu$ -SXRF).* A polished section of the mine waste sample was mapped for elemental distribution using the  $\mu$ -SXRF beam line (BL) 10-2 at the Stanford Synchrotron Radiation Light Source (SSRL). The maps were collected using a Si (111) phi, 90 double crystal monochromator at a 50  $\mu$ m resolution upto 17200 eV X-ray energies, just above the U L<sub>III</sub> edge. All data processing was conducted using the Microanalysis Toolkit software program.

*Reactive Transport Modelling (PFLOTRAN).* Below are the supporting equations that were used in PFLOTRAN to calculate the change in concentration while taking the dominant processes into account. The total aqueous concentrations ( $\Psi_j$ ) [ $\text{ML}^{-3}$ ] for a particular species j is given by equation [2], where  $C_j$  and  $C_i$  [ $\text{ML}^{-3}$ ] represent concentrations of j<sup>th</sup> primary species from 1 to  $N_c$  and i<sup>th</sup> secondary species that varies from 1 to  $N_{sec}$  in the liquid phase.

$$\Psi_j = C_j + \sum_{i=1}^{N_{sec}} v_{ji} C_i \quad (2)$$

The secondary species concentrations ( $C_i$ ) are estimated in terms of primary species concentration using equation [3] with known values of equilibrium constant  $K_{eq_i}$  [-], and activity coefficients  $\gamma_i$  and  $\gamma_j$  that are computed using the Debye-Hückel equation that,

$$C_i = (\gamma_i)^{-1} K_{eq_i} \prod_{j=1}^{N_c} (\gamma_j C_j)^{v_{ji}} \quad (3)$$

Correspond to the homogeneous aqueous reactions described in equation [4a] and [4b].



These reactions are written in their canonical form where  $A_j$  denotes the primary species,  $A_i$  aqueous secondary species,  $v_{ji}$  and  $v_{jm}$  [-] stoichiometric coefficient for aqueous and mineral reactions respectively, and  $M_m$  denotes minerals.<sup>1</sup> The reaction rate ( $I_m$ ) [ $\text{ML}^{-3}\text{T}^{-1}$ ] is given by equation [5] based on the transition state theory where  $Q_{IAP_m}$  [ $\text{M L}^{-3}\text{T}^{-1}$ ] is the ion activity product [6],  $a_m$  [ $\text{L}^{-1}$ ] is the new specific surface area that is a function of porosity ( $\varphi$ ),  $k_m$  is reaction rate constant,  $P_m$  [-] is a prefactor that accounts for the pH dependence and  $\zeta_m$  [-] is a factor whose value is 0 or 1 depending if  $K_{eq_m} Q_{IAP_m} \leq 1$  and  $\varphi_m = 0$  or  $K_{eq_m} Q_{IAP_m} > 1$  and  $n_m$  [-] is fitting parameter.<sup>2</sup> Water-rock reactions typically follow a non-linear rate law that is sensitive to this fitting parameter ‘ $n_m$ ’ in PFLOTRAN.<sup>2, 3 4</sup>

$$I_m = -k_m a_m P_m (1 - (K_{eq_m} Q_{IAP_m})^{n_m}) \zeta_m \quad (5)$$

$$Q_m = \prod_{k=1}^{N_c} (\gamma_k^l C_k^l)^{v_{km}} \quad (6)$$

The sign convention used in PFLOTRAN is that if the rate is positive the mineral is precipitating and if it is negative the mineral is dissolving. The change in the material properties like porosity  $\varphi$  and surface area  $a_m$  due to mineral precipitation and dissolution reactions are accounted through equations [7] and [8], where,  $\varphi_m$  [-],  $\phi_m$  [-],  $\phi_m^0$  [-] and  $a_m^o$  [ $L^{-1}$ ] denote porosity of the  $m^{\text{th}}$  mineral, volume fraction of the  $m^{\text{th}}$  mineral, initial volume fraction of the  $m^{\text{th}}$  mineral and initial mineral specific surface area.

$$\varphi = 1 - \sum_m \varphi_m \quad (7)$$

$$a_m = a_m^o \left( \frac{\phi_m}{\phi_m^0} \right)^{n_m} \quad (8)$$

The porosity,  $\varphi = 0.25$ , of the Blue Gap/Tachee mine waste sediments were estimated using equation [9] where the bulk density ( $\rho_b = 1.65 \text{ gm cm}^{-3}$  [ $ML^{-3}$ ]) and particle density ( $\rho_p = 2.25 \text{ gm cm}^{-3}$  [ $ML^{-3}$ ]) were acquired experimentally.

$$\varphi = 1 - \frac{\rho_b}{\rho_p} \quad (9)$$

However, other material properties like tortuosity ( $\tau$ ) and aqueous diffusion coefficient [ $M^2T^{-1}$ ] were assumed to be,  $\tau = 1$  and  $10^{-9} \text{ m}^2 \text{ s}^{-1}$  respectively. The assumption for tortuosity was made for simplification purposes, while the assumption for aqueous diffusion coefficient was made based on the diffusion coefficients of  $H^+$ ,  $CO_3^{2-}$ ,  $HCO_3^-$ ,  $Ca_2UO_2(CO_3)_3^0$ ,  $CaUO_2(CO_3)_3^{2-}$ ,  $UO_2(CO_3)_2^{2-}$  and  $Ca^{2+}$  that were all found to be around  $10^{-9} \text{ m}^2 \text{ s}^{-1}$  at  $25^\circ C$ .<sup>5,6</sup> The dirichlet initial and boundary conditions were imposed on the 1D reactive transport of metals over time during reaction with  $10 \text{ mM } HCO_3^-$  and  $10 \text{ mM } CH_3COOH$ . The initial surface area  $a_m^o$  ( $L^{-1}$ ) of U-V

bearing minerals in the mine waste sediments is calculated using equation [10] in  $\text{cm}^2 \text{cm}^{-3}$ . The specific mineral surface area  $a_m^o$ , [ $\text{L}^{-1}$ ] is defined as

$$a_m^o = \frac{A_m}{V} = \frac{A_m V_m}{V_m V} = \frac{a_m}{v_m} \phi_m \quad (10)$$

where  $\phi_m = V_m/V$  and  $V_m$  are the volume fraction and volume of the  $m^{\text{th}}$  mineral contained in the REV of volume  $V$ , respectively, and  $a_m$  [ $\text{L}^{-1}$ ] and  $v_m$  [ $\text{L}^3$ ] refer to the area and volume of a single sphere of radius  $r_m$  [ $\text{L}$ ],

$$a_m = 4\pi r_m^2 \quad (11)$$

$$v_m = \frac{4}{3}\pi r_m^3 \quad (12)$$

Thus the surface area  $a_m^o$  [ $\text{L}^{-1}$ ] further simplifies to,

$$a_m^o = \frac{3}{r_m} \phi_m \quad (13)$$

The surface area of the U-V bearing mineral was estimated using equation [13] by considering the average particle size of the mine waste used in batch ( $<63 \mu\text{m}$ ) and column ( $120\text{-}355 \mu\text{m}$ ) based on the assumption that 1) all of the U-phases in the mine waste are U-V bearing minerals and 2) the U-V bearing minerals are spherical in shape. The assumptions were made based on prior knowledge on the Blue Gap/Tachee mine site,<sup>7</sup> where U-V bearing mineral was identified as the dominant U-phase in the mine waste. The shape of the U-V bearing minerals was assumed to be spherical for simplifying the calculations.



**Table S1.** Thermodynamic equilibrium constants (at T = 25°C) for aqueous and solid phase U(VI) used in the reactive transport model (PFLOTTRAN).

U(VI) Aqueous and Mineral species	Log $K_{eq}$	Reference	Implementation in the model
<b>Primary species</b>			
$H_2O = OH^- + H^+$	-14.00	Shock et al., 1988 <sup>8,9</sup>	Fixed
$U^{4+} + 1.5 H_2O + 0.25O_2 = UO_2^{2+} + 3 H^+$	-13.2076	Cox et al., 1989 <sup>10</sup>	Fixed
$VO^{2+} + 0.5 H_2O + 0.5O_2 = VO^{2+} + H^+$	-3.8528	Shock et al., 1988 <sup>8</sup>	Fixed
$H_3AsO_4 + H^+ = H_2AsO_4^-$	2.2492	Shock et al., 1988 <sup>8</sup>	Fixed
$H_2CO_3 = HCO_3^- + H^+$	6.37	Shock et al., 1988 <sup>8</sup>	Fixed
$HCO_3^- = CO_3^{2-} + H^+$	10.33	Shock et al., 1988 <sup>8</sup>	Fixed
$HCO_3^- + H^+ = H_2O + CO_2 (aq)$	-6.3447	Shock et al., 1988 <sup>8</sup>	Fixed
<b>Aqueous complexes</b>			
$Al^{3+} + H_2O = AlOH^{2+} + H^+$	4.971	Pokrovskii et al., 1995 <sup>11</sup>	Fixed
$Al^{3+} + 2H_2O = Al(OH)_2^+ + H^+$	10.594	Pokrovskii et al., 1995 <sup>11</sup>	Fixed
$Al^{3+} + 3H_2O = Al(OH)_3 (aq) + 3H^+$	16.1577	Pokrovskii et al., 1995 <sup>11</sup>	Fixed
$Al^{3+} + 4H_2O = Al(OH)_4^- + H^+$	22.8833	Pokrovskii et al., 1995 <sup>11</sup>	Fixed
$Ca^{2+} + H_2O = CaOH^+ + H^+$	12.85	Baes et al., 1976 <sup>12</sup>	Fixed
$Ca^{2+} + HCO_3^- = CaCO_3 (aq) + H^+$	7.0017	Johnson. J. W et al. 1992 <sup>13</sup>	Fixed
$Ca^{2+} + HCO_3^- = CaHCO_3^+$	-1.0467	Johnson. J. W et al. 1992 <sup>13</sup>	Fixed
$Mg^{2+} + OH^- = MgOH^+$	-2.210	Johnson. J. W et al. 1992 <sup>13</sup>	Fixed
$Mg^{2+} + HCO_3^- = MgCO_3 (aq) + H^+$	7.3499	Johnson. J. W et al. 1992 <sup>13</sup>	Fixed
$Mg^{2+} + HCO_3^- = MgHCO_3^+$	-1.0357	Johnson. J. W et al. 1992 <sup>13</sup>	Fixed

$\text{Mn}^{2+} + \text{H}_2\text{O} = \text{MnOH}^+ + \text{H}^+$	10.59	Baes et al., 1976 <sup>12</sup>	Fixed
$\text{Mn}^{2+} + 3\text{H}_2\text{O} = \text{Mn}(\text{OH})_3^- + 3\text{H}^+$	34.22	Wagman et al., 1982 <sup>14</sup>	Fixed
$\text{Mn}^{2+} + 4\text{H}_2\text{O} = \text{Mn}(\text{OH})_4^{2-} + 4\text{H}^+$	48.3	Baes et al., 1976 <sup>12</sup>	Fixed
$\text{Na}^+ + \text{H}_2\text{O} = \text{NaOH}(\text{aq}) + \text{H}^+$	14.79	Johnson. J. W et al. 1992 <sup>13</sup>	Fixed
$\text{Na}^+ + \text{HCO}_3^- = \text{NaHCO}_3(\text{aq})$	-0.1541	Wagman et al., 1982 <sup>14</sup>	Fixed
$\text{K}^+ + \text{H}_2\text{O} = \text{KOH}(\text{aq}) + \text{H}^+$	14.46	Baes et al., 1976 <sup>12</sup>	Fixed
$\text{H}^+ + \text{SO}_4^{2-} = \text{HS}^- + 2\text{O}_2$	132.52	Shock et al., 1988 <sup>8</sup>	Fixed
$\text{Fe}^{2+} + \text{H}^+ + 0.25 \text{O}_2 = \text{Fe}^{3+} + 0.5 \text{H}_2\text{O}$	-7.765	Shock et al., 1988 <sup>8</sup>	Fixed
$\text{Fe}^{2+} + \text{H}_2\text{O} = \text{FeOH}^+ + \text{H}^+$	9.5	Baes et al., 1976 <sup>12</sup>	Fixed
$\text{Fe}^{2+} + 2\text{H}_2\text{O} = \text{Fe}(\text{OH})_2(\text{aq}) + \text{H}^+$	20.60	Baes et al., 1976 <sup>12</sup>	Fixed
$\text{Fe}^{3+} + 2\text{H}_2\text{O} = \text{Fe}(\text{OH})_2^+ + 2\text{H}^+$	5.67	Baes et al., 1976 <sup>12</sup>	Fixed
$\text{Fe}^{3+} + 3\text{H}_2\text{O} = \text{Fe}(\text{OH})_3(\text{aq}) + 3\text{H}^+$	12	Baes et al., 1976 <sup>12</sup>	Fixed
$\text{Fe}^{2+} + 3\text{H}_2\text{O} = \text{Fe}(\text{OH})_3^- + 3\text{H}^+$	31	Baes et al., 1976 <sup>12</sup>	Fixed
$\text{Fe}^{3+} + 4\text{H}_2\text{O} = \text{Fe}(\text{OH})_4^- + 4\text{H}^+$	21.6	Baes et al., 1976 <sup>12</sup>	Fixed
$\text{Fe}^{2+} + 4\text{H}_2\text{O} = \text{Fe}(\text{OH})_4^{2-} + 4\text{H}^+$	46	Baes et al., 1976 <sup>12</sup>	Fixed
$\text{Fe}^{2+} + \text{CO}_3^{2-} = \text{FeCO}_3(\text{aq})$	5.5988	Turner et al., 1981 <sup>15</sup>	Fixed
$\text{Fe}^{2+} + \text{HCO}_3^- = \text{FeCO}_3^+ + \text{H}^+$	0.6088	Turner et al., 1981 <sup>15</sup>	Fixed
$\text{Fe}^{2+} + \text{HCO}_3^- = \text{FeHCO}_3^+$	-2.72	Mattigod et al., 1979 <sup>16</sup>	Fixed
$\text{Li}^+ + \text{H}_2\text{O} = \text{LiOH}(\text{aq}) + \text{H}^+$	13.64	Baes et al., 1976 <sup>12</sup>	Fixed
$\text{UO}_2^{2+} + \text{H}^+ = \text{U}^{3+} + 0.75\text{O}_2 + 0.5\text{H}_2\text{O}$	62.6291	Grenthe et al., 1992 <sup>17</sup>	Fixed
$\text{UO}_2^{2+} + 2\text{H}^+ = \text{U}^{4+} + \text{H}_2\text{O} + 0.5\text{O}_2$	32.4999	Grenthe et al., 1992 <sup>17</sup>	Fixed
$\text{U}^{4+} + 1.5\text{H}_2\text{O} + 0.25\text{O}_2 = \text{UO}_2^{2+} + 3\text{H}^+$	-13.2076	Grenthe et al., 1992 <sup>17</sup>	Fixed

$\text{UO}_2^{2+} + \text{H}_2\text{O} = \text{UO}_2\text{OH}^+ + \text{H}^+$	5.2073	Grenthe et al., 1992 <sup>17</sup>	Fixed
$\text{UO}_2^{2+} + 2\text{H}_2\text{O} = \text{UO}_2(\text{OH})_2 (\text{aq}) + 2\text{H}^+$	10.3146	Grenthe et al., 1992 <sup>17</sup>	Fixed
$\text{UO}_2^{2+} + 3\text{H}_2\text{O} = \text{UO}_2(\text{OH})_3^- + 3\text{H}^+$	19.2218	Grenthe et al., 1992 <sup>17</sup>	Fixed
$\text{UO}_2^{2+} + 4\text{H}_2\text{O} = \text{UO}_2(\text{OH})_4^{2-} + 4\text{H}^+$	33.0291	Grenthe et al., 1992 <sup>17</sup>	Fixed
$2\text{UO}_2^{2+} + 1\text{H}_2\text{O} = (\text{UO}_2)_2\text{OH}^{3+} + \text{H}^+$	2.7072	Grenthe et al., 1992 <sup>17</sup>	Fixed
$2\text{UO}_2^{2+} + 2\text{H}_2\text{O} = (\text{UO}_2)_2(\text{OH})_2^{2+} + 2\text{H}^+$	5.6346	Grenthe et al., 1992 <sup>17</sup>	Fixed
$3\text{UO}_2^{2+} + 4\text{H}_2\text{O} = (\text{UO}_2)_3(\text{OH})_4^{2+} + 4\text{H}^+$	11.929	Grenthe et al., 1992 <sup>17</sup>	Fixed
$3\text{UO}_2^{2+} + 5\text{H}_2\text{O} = (\text{UO}_2)_3(\text{OH})_5^+ + 5\text{H}^+$	15.5862	Grenthe et al., 1992 <sup>17</sup>	Fixed
$3\text{UO}_2^{2+} + 7\text{H}_2\text{O} = ((\text{UO}_2)_3(\text{OH})_7^- + 7\text{H}^+$	31.0508	Grenthe et al., 1992 <sup>17</sup>	Fixed
$4\text{UO}_2^{2+} + 7\text{H}_2\text{O} = (\text{UO}_2)_4(\text{OH})_7^+ + 7\text{H}^+$	21.9508	Grenthe et al., 1992 <sup>17</sup>	Fixed
$\text{UO}_2^{2+} + \text{HCO}_3^- = \text{UO}_2\text{CO}_3(\text{aq}) + \text{H}^+$	0.6634	Grenthe et al., 1992 <sup>17</sup>	Fixed
$\text{UO}_2^{2+} + 2\text{HCO}_3^- = \text{UO}_2(\text{CO}_3)_2^{2-} + 2\text{H}^+$	3.7467	Grenthe et al., 1992 <sup>17</sup>	Fixed
$\text{UO}_2^{2+} + 3\text{HCO}_3^- = \text{UO}_2(\text{CO}_3)_3^{4-} + 3\text{H}^+$	9.4302	Grenthe et al., 1992 <sup>17</sup>	Fixed
$2\text{UO}_2^{2+} + 3\text{H}_2\text{O} + \text{HCO}_3^- =$ $(\text{UO}_2)_2\text{CO}_3(\text{OH})_3^- + 4\text{H}^+$	11.2229	Grenthe et al., 1992 <sup>17</sup>	Fixed
$2\text{Ca}^{2+} + \text{UO}_2^{2+} + 3\text{CO}_3^{2-} = \text{Ca}_2\text{UO}_2(\text{CO}_3)_3$ $(\text{aq})$	-30.04	Dong et al., 2006 <sup>18</sup>	Fixed
$\text{Ca}^{2+} + \text{UO}_2^{2+} + 3\text{CO}_3^{2-} = \text{CaUO}_2(\text{CO}_3)_3^{2-}$	-27.18	Dong et al., 2006 <sup>18</sup> , Bernhard et al., 2001 <sup>19</sup>	Fixed
$\text{VO}^{2+} + \text{H}^+ = \text{V}^{3+} + 0.5\text{H}_2\text{O} + 0.25\text{O}_2$	14.9945	Israel et al., 1976 <sup>20</sup>	Fixed
$\text{VO}^{2+} + 0.5\text{H}_2\text{O} + 0.25\text{O}_2 = \text{VO}_2^+ + \text{H}^+$	-3.8528	Shock et al., 1988 <sup>8</sup>	Fixed
$\text{V}^{3+} + 3\text{H}_2\text{O} + 0.5\text{O}_2 = \text{VO}_4^{3-} + 6\text{H}^+$	9.6002	Wagman et al., 1982 <sup>14</sup>	Fixed
$\text{VO}^{2+} + 2\text{H}_2\text{O} = (\text{VO})_2(\text{OH})_2^{2+} + 2\text{H}^+$	6.67	Baes et al., 1976 <sup>12</sup>	Fixed
$\text{VO}^{2+} + 2.5\text{H}_2\text{O} + 0.25\text{O}_2 = \text{H}_2\text{VO}_4^- + 3\text{H}^+$	3.2394	Johnson. J. W et al. 1992 <sup>13</sup>	Fixed
$\text{VO}^{2+} + 2.5\text{H}_2\text{O} + 0.25\text{O}_2 = \text{HVO}_4^{2-} + 4\text{H}^+$	11.3024	Johnson. J. W et al. 1992 <sup>13</sup>	Fixed

$V^{3+} + H_2O = VOH^{2+} + H^+$	2.260	Baes et al., 1976 <sup>12</sup>	Fixed
$VO^{2+} + H_2O = VOOH^+ + H^+$	5.67	Baes et al., 1976 <sup>12</sup>	Fixed
$VO_4^{3-} + 2H^+ = VO_3OH^{2-}$	-14.26	Baes et al., 1976 <sup>12</sup>	Fixed
$V^{3+} + 2H_2O = V(OH)_2^+ + 2H^+$	5.9193	Langmuir et al., 1978 <sup>21</sup>	Fixed
$2V^{3+} + 2H_2O = V_2(OH)_2^{4+} + 2H^+$	3.80	Baes et al., 1976 <sup>12</sup>	Fixed
$VO_2^+ + 2H_2O = VO(OH)_3(aq) + H^+$	3.30	Baes et al., 1976 <sup>12</sup>	Fixed
$H_2AsO_4^- + H^+ = AsH_3(aq) + 2O_2$	149.3941	Sergeyeva et al., 1969 <sup>22</sup>	Fixed
$H_2AsO_4^- = H_2AsO_3^- + 0.5O_2$	29.0857	Shock et al., 1988 <sup>8</sup>	Fixed
$H_2AsO_4^- = AsO_2^- + 3H_2O + 0.5O_2$	29.0746	Grenthe et al., 1992 <sup>17</sup>	Fixed
$H_2AsO_3^- + 4H^+ = As(OH)_3(aq)$	-9.2048	Grenthe et al., 1992 <sup>17</sup>	Fixed
<b>Solid Mineral phases</b>			
Calcite $CaCO_3 + H^+ = Ca^{2+} + HCO_3^-$	1.8487	Helgeson et al. 1978 <sup>23</sup>	Fixed
Becquerelite $Ca(UO_2)_6O_4(OH)_6 \cdot 8H_2O + 14H^+ = 6UO_2^{2+} + Ca^{2+} + 18H_2O$	29.23	Casas et al., 1997 <sup>24</sup>	Fixed
Quartz $SiO_2 = SiO_2(aq)$	-3.9993	Helgeson et al. 1978 <sup>23</sup>	Fixed
Boehmite $AlO_2H + 3H^+ = Al^{3+} + 2H_2O$	7.5642	Pokrovskii et al., 1995 <sup>11</sup>	Fixed
Diaspore $AlHO_2 + 3H^+ = Al^{3+} + 2H_2O$	7.1603	Pokrovskii et al., 1995 <sup>11</sup>	Fixed
Gibbsite $Al(OH)_3 + 3H^+ = Al^{3+} + 3H_2O$	7.756	Pokrovskii et al., 1995 <sup>11</sup>	Fixed
Hercynite $FeAl_2O_4 + 8H^+ = Fe^{2+} + 2Al^{3+} + 4H_2O$	28.8484	Robie et al. 1995 <sup>25</sup>	Fixed
Spinel $Al_2MgO_4 + 8H^+ = Mg^{2+} + 2Al^{3+} + 4H_2O$	37.6295	Helgeson et al. 1978 <sup>23</sup>	Fixed

Portlandite $\text{Ca}(\text{OH})_2 + 2\text{H}^+ = \text{Ca}^{2+} + 2\text{H}_2\text{O}$	22.5552	Robie et al. 1995 <sup>25</sup>	Fixed
Wustite $\text{Fe}_{0.947}\text{O} + 2\text{H}^+ = 0.1060\text{Fe}^{3+} + 0.8410\text{Fe}^{2+} + \text{H}_2\text{O}$	12.4113	Wagman et al., 1982 <sup>14</sup>	Fixed
Periclase $\text{MgO} + 2\text{H}^+ = \text{Mg}^{2+} + \text{H}_2\text{O}$	21.3354	Helgeson et al. 1978 <sup>23</sup>	Fixed
Brucite $\text{Mg}(\text{OH})_2 + 2\text{H}^+ = \text{Mg}^{2+} + 2\text{H}_2\text{O}$	16.2980	Helgeson et al. 1978 <sup>23</sup>	Fixed
Ferrihydrite $\text{Fe}_2\text{O}_3 + 3\text{H}^+ = \text{Fe}^{3+} + 3\text{H}_2\text{O}$	4.896	Stumm and Morgan <sup>26</sup>	Fixed
Goethite $\text{FeOOH} + 3\text{H}^+ = \text{Fe}^{3+} + 2\text{H}_2\text{O}$	0.5345	Robie et al. 1995 <sup>25</sup>	Fixed
Hematite $\text{Fe}_2\text{O}_3 + 6\text{H}^+ = 2\text{Fe}^{3+} + 3\text{H}_2\text{O}$	0.1086	Helgeson et al. 1978 <sup>23</sup>	Fixed
Uraninite $\text{UO}_2 + 4\text{H}^+ = \text{U}^{4+} + 2\text{H}_2\text{O}$	-4.8372	Cox et al., 1989 <sup>10</sup>	Fixed
Schoepite $\text{UO}_3 \cdot 2\text{H}_2\text{O} + 2\text{H}^+ = \text{UO}_2^{2+} + 3\text{H}_2\text{O}$	4.8333	Grenthe et al., 1992 <sup>17</sup>	Fixed
Rutherfordine $\text{UO}_2\text{CO}_3 + \text{H}^+ = \text{HCO}_3^- + \text{UO}_2^{2+}$	-13.9	Meinrath 1993 <sup>27</sup>	Fixed
Boltwoodite-Na $\text{Na}_{.7}\text{K}_{.3}(\text{H}_3\text{O})(\text{UO}_2)\text{SiO}_4 \cdot \text{H}_2\text{O} + 3\text{H}^+ = 0.3\text{K}^+ + 0.7\text{Na}^+ + \text{SiO}_2(\text{aq})$	14.5834	Hemingway et al., 1982	Fixed
Metaschoepite $\text{UO}_3 \cdot 2\text{H}_2\text{O} + 2\text{H}^+ = \text{UO}_2^{2+} + 3\text{H}_2\text{O}$	-22.29 (circumneutral), -5.26 (acidic)	Meinrath 1993 <sup>27</sup> , Riba et al., 2005 <sup>28</sup>	Fixed
Uranophane $\text{Ca}(\text{UO}_2)_2(\text{SiO}_3)_2(\text{OH})_2 + 6\text{H}^+ = \text{Ca}^{2+} + 2\text{SiO}_2$	17.2850	Wagman et al., 1982 <sup>14</sup>	Fixed
$\text{UO}_2\text{CO}_3 + \text{H}^+ = \text{HCO}_3^- + \text{UO}_2^{2+}$	-4.1267	Grenthe et al., 1992 <sup>17</sup>	Fixed
$\text{CaUO}_4 + 4\text{H}^+ = \text{Ca}^{2+} + \text{UO}_2^{2+} + 2\text{H}_2\text{O}$	15.9420	Grenthe et al., 1992 <sup>17</sup>	Fixed
$\text{UO}_3 \cdot 2\text{H}_2\text{O} + 2\text{H}^+ = \text{UO}_2^{2+} + 3\text{H}_2\text{O}$	4.833	Grenthe et al., 1992 <sup>17</sup>	Fixed
Schoepite-dehydrated $0.9\text{UO}_3 \cdot 0.9\text{H}_2\text{O} + 2\text{H}^+ = \text{UO}_2^{2+} + 1.9\text{H}_2\text{O}$	5.0167	Grenthe et al., 1992 <sup>17</sup>	Fixed

$V_2O_4 + 4H^+ = 2H_2O + 2VO^{2+}$	8.5719	Wagman et al., 1982 <sup>14</sup>	Fixed
$V_3O_5 + 8H^+ = VO^{2+} + 2V^{3+} + 4H_2O$	13.4312	Wagman et al., 1982 <sup>14</sup>	Fixed
$V_4O_7 + 10H^+ = 2V^{3+} + 2VO^{2+} + 5H_2O$	18.7946	Wagman et al., 1982 <sup>14</sup>	Fixed
<i>Carnotite</i> $(K_2(UO_2)_2(VO_4)_2)^* = 2K^+ + 2UO_2^{2+} + 2VO_4^{3-}$	-56.3811	<i>Langmuir et al., 1978</i> <sup>21</sup>	<i>Varied</i>
$Mg_2V_2O_7 + H_2O = 2H^+ + 2Mg^{2+} + 2VO_4^{3-}$	-30.9025	Wagman et al., 1982 <sup>14</sup>	Fixed
$MgV_2O_6 + 2H_2O = Mg^{2+} + 2VO_4^{3-} + 4H^+$	-45.8458	Wagman et al., 1982 <sup>14</sup>	Fixed
<i>Tyuyamunite</i> $Ca(UO_2)_2(VO_4)_2 = Ca^{2+} + 2UO_2^{2+} + 2VO_4^{3-}$	-53.3757	Langmuir et al., 1978 <sup>21</sup>	Fixed
<i>Arsenopyrite</i> $FeAsS + 1.5H_2O = 0.5H^+ + 0.5AsH_3(aq)$	-14.4453	Wagman et al., 1982 <sup>14</sup>	Fixed
<i>Arsenolite</i> $As_2O_3 + 3H_2O = 2H^+ + 2H_2AsO_3^-$	-19.8365	Robie et al. 1995 <sup>25</sup>	Fixed
$(UO_2)_2As_2O_7 + 2H^+ + H_2O = 2H_2AsO_4^- + 2UO_2^{2+}$	7.7066	Grenthe et al., 1992 <sup>17</sup>	Fixed
$(UO_2)_3(AsO_4)_2 + 4H^+ = 2H_2AsO_4^- + 3UO_2^{2+}$	9.3177	Grenthe et al., 1992 <sup>17</sup>	Fixed
$KUO_2AsO_4 + 2H^+ = H_2AsO_4^- + K^+ + UO_2^{2+}$	-4.1741	Wagman et al., 1982 <sup>14</sup>	Fixed
$LiUO_2AsO_4 + 2H^+ = H_2AsO_4^- + Li^+ + UO_2^{2+}$	-0.7862	Wagman et al., 1982 <sup>14</sup>	Fixed
$UO_2(AsO_3)_2 + 2H_2O = UO_2^{2+} + 2H_2AsO_4^-$	6.9377	Grenthe et al., 1992 <sup>17</sup>	Fixed
<b>Surface Complexes</b>			
$>SOUO_2OH$	6.448	Bond et al., 2007 <sup>29</sup>	Fixed
$>SOHUO_2CO_3$	2.033	Bond et al., 2007 <sup>29</sup>	Fixed

**Table S2.** Other parameters used in the reactive transport model to simulate the experimental release of U and V from mine waste.

Parameter	Value	Implementation in the model
Reaction rate constant ( $k_m$ ) of carnotite	-	Varied
Reaction rate constant ( $k_m$ ) of Rutherfordine (UO <sub>2</sub> CO <sub>3</sub> ) (mol cm <sup>-2</sup> sec <sup>-1</sup> )	-	Varied
Reaction rate constant ( $k_m$ ) of metaschoepite (UO <sub>3</sub> ·2H <sub>2</sub> O) (mol cm <sup>-2</sup> sec <sup>-1</sup> )	-	Varied
Porosity ( $\phi$ )	0.25	Calculated, Fixed
Tortuosity (tau)	1	Assumed, Fixed
aqueous diffusion coefficient (m <sup>2</sup> s <sup>-1</sup> )	10 <sup>-9</sup>	From Literature, Fixed
Darcy's Flux, $q$ (cm min <sup>-1</sup> )	1.496	Calculated, Fixed
Average U-V bearing mineral diameter ( $\mu$ m) Batch experiments (<63 $\mu$ m)	32	Assumed based on size fractions to calculate average surface area, fixed
Average U-V bearing mineral diameter ( $\mu$ m) Column Experiments (120-355 $\mu$ m)	240	Assumed based on size fractions to calculate average surface area, fixed

**Table S3.** Reaction rate constants of metaschoepite and rutherfordine estimated by modelling the reactive transport of U and V during mine waste reaction at circumneutral and acidic conditions.

<b>Mineral phase</b>	<b>Reaction rate constants (<math>k_m</math>) (mol cm<sup>-2</sup> sec<sup>-1</sup>)</b>
Rutherfordine (UO <sub>2</sub> CO <sub>3</sub> ) (Circumneutral Batch)	1x10 <sup>-15</sup>
Metaschoepite (UO <sub>3</sub> .2H <sub>2</sub> O) (Circumneutral Batch)	2x10 <sup>-16</sup>



**Table S4.** Parameters used to consider the effect of grain size on the reactive transport of U and V during flow through column experiment with 10 mM HCO<sub>3</sub><sup>-</sup>. The surface area of U-V bearing minerals was estimated using equation 13. The effective reaction rate constant ( $k_{effective} = k * a_m^0$ ) accounts for the effect of grain surface area on the reactive transport of U and V, where  $k$  is the reaction rate constant and  $a_m^0$  is the surface area of U-V bearing minerals.

<b>U-V bearing minerals of different grain sizes</b>	<b>Average U-V bearing mineral diameter (μm)</b>	<b>Estimated U-V bearing mineral surface area (<math>a_m^0</math>) (cm<sup>2</sup> cm<sup>-3</sup>)</b>	<b>Reaction rate constant (<math>k_m</math>) (mol cm<sup>-2</sup> sec<sup>-1</sup>)</b>	<b>Effective reaction rate constant (<math>k_{effective} = (k_m * a_m^0)</math>) (mol cm<sup>-3</sup> sec<sup>-1</sup>)</b>
U-V mineral	240	62.5	4.8x10 <sup>-13</sup>	3.0x10 <sup>-11</sup>
U-V mineral 1	200	75	4.8x10 <sup>-13</sup>	3.6x10 <sup>-11</sup>
U-V mineral 2	280	53.6	4.8x10 <sup>-13</sup>	2.6x10 <sup>-11</sup>
U-V mineral 3	120	125	4.8x10 <sup>-13</sup>	6.0x10 <sup>-11</sup>

**Table S5.** Elemental content of solid samples determined by acid extractions (measured using ICP-OES/MS) of unreacted mine waste and mine waste after sequential reaction with 10 mM  $\text{HCO}_3^-$  and  $\text{CH}_3\text{COOH}$  solution during flow through column experiments.

<b>Samples</b>	<b>U (mg Kg<sup>-1</sup>)</b>	<b>V (mg Kg<sup>-1</sup>)</b>	<b>As (mg Kg<sup>-1</sup>)</b>	<b>Fe (mg Kg<sup>-1</sup>)</b>
Unreacted mine waste Acid extractable	1912.12	858.01	4.015	715.79
Reacted mine waste Acid extractable	17.79	62.01	1.17	456.89

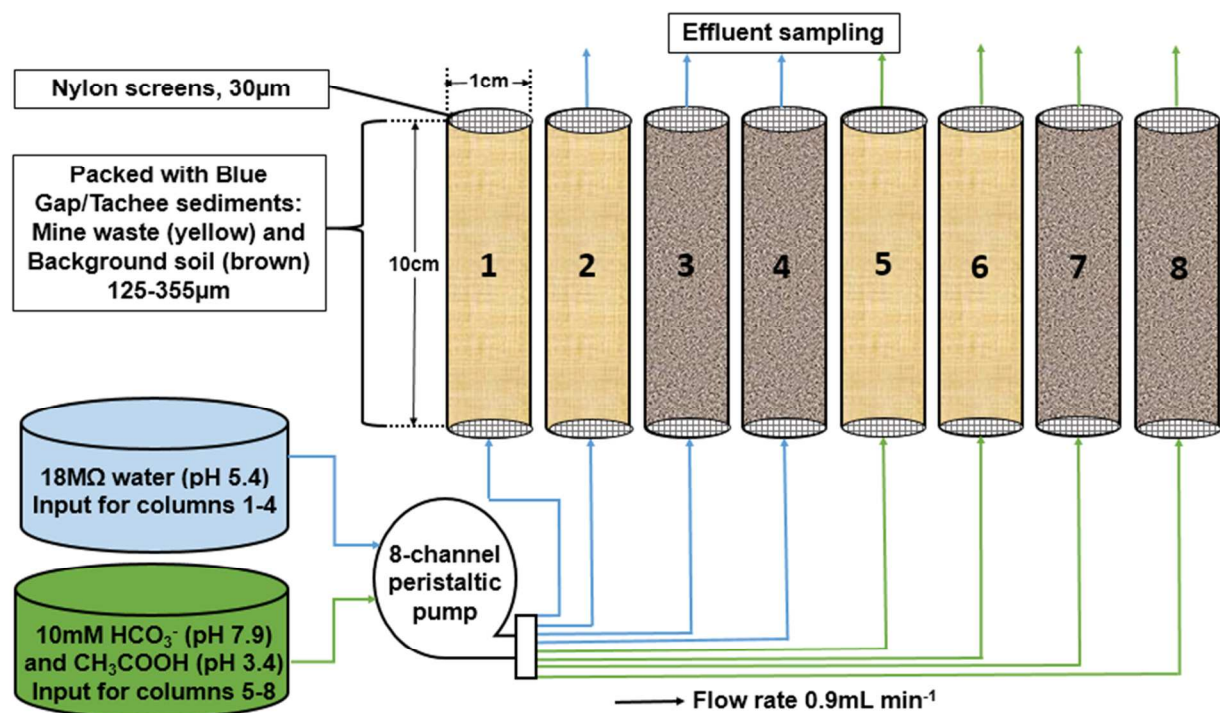


**Figure S1.** Experimental setup of sequential flow through column experiments

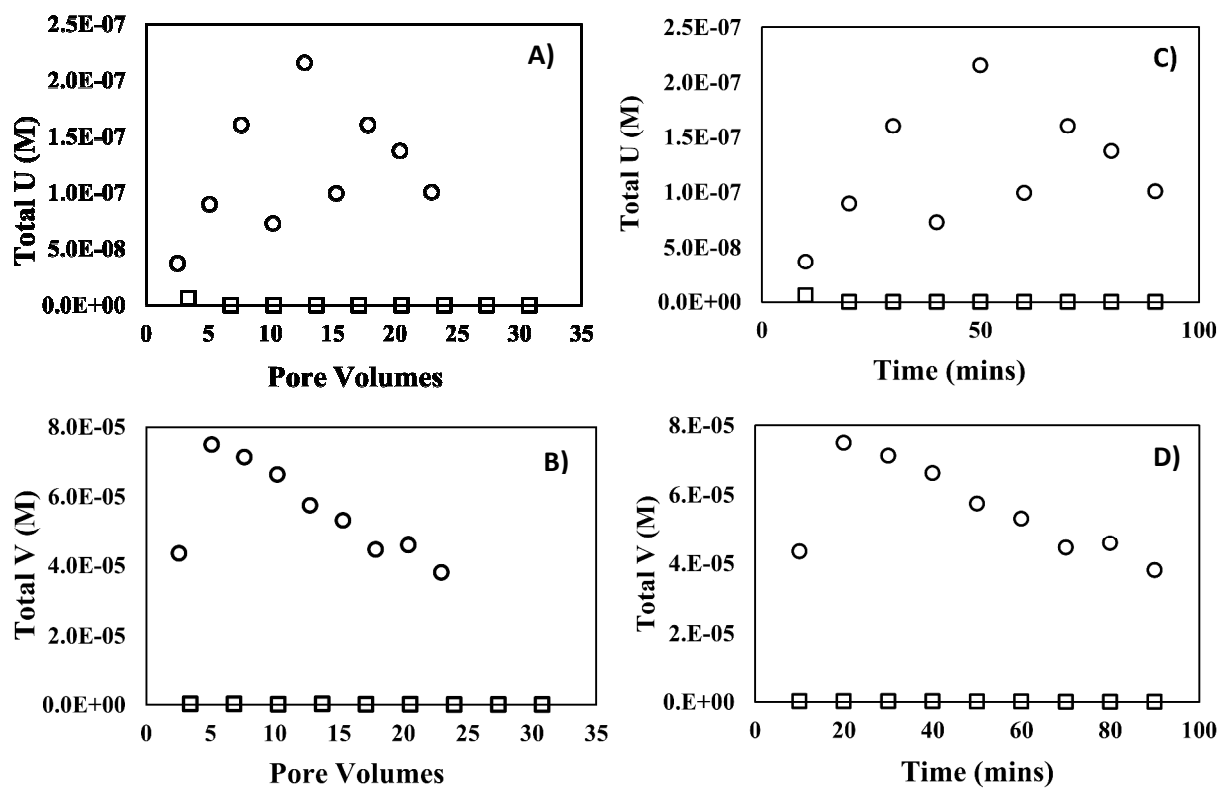


**Figure S2.** Effluent concentrations of U and V obtained after reaction of mine waste (circle) and background soil (squares) with 18MΩ water (pH 5.4), during continuous flow-through column experiments, as a function of pore volumes and time. **A)** U concentration versus pore volume; **B)** V concentration versus pore volume; **C)** U concentration versus time; **D)** V concentration versus time.

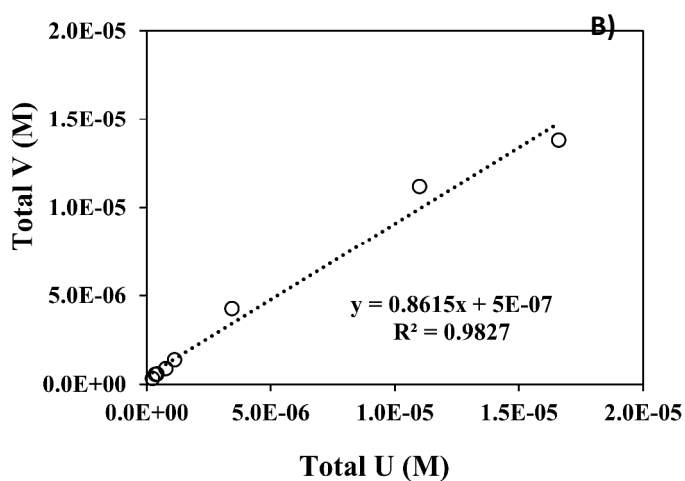
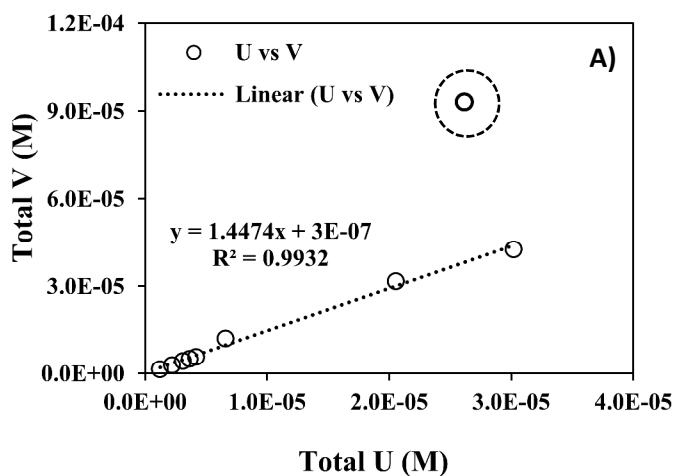


**Figure S3.** Molar correlation between U and V experimental release from mine waste (hollow circles) after reaction with **A)** 10 mM HCO<sub>3</sub><sup>-</sup> and **B)** 10 mM CH<sub>3</sub>COOH during continuous flow through column experiments. The ideal slope should be 1:1 from the reaction  $(K_2(UO_2)_2(VO_4)_2)^* = 2K^+ + 2UO_2^{2+} + 2VO_4^{3-}$ . The point in the dashed circle represents an outlier due to equilibration of the column with the influent solution on the early stages of the experiment (first 30 minutes).

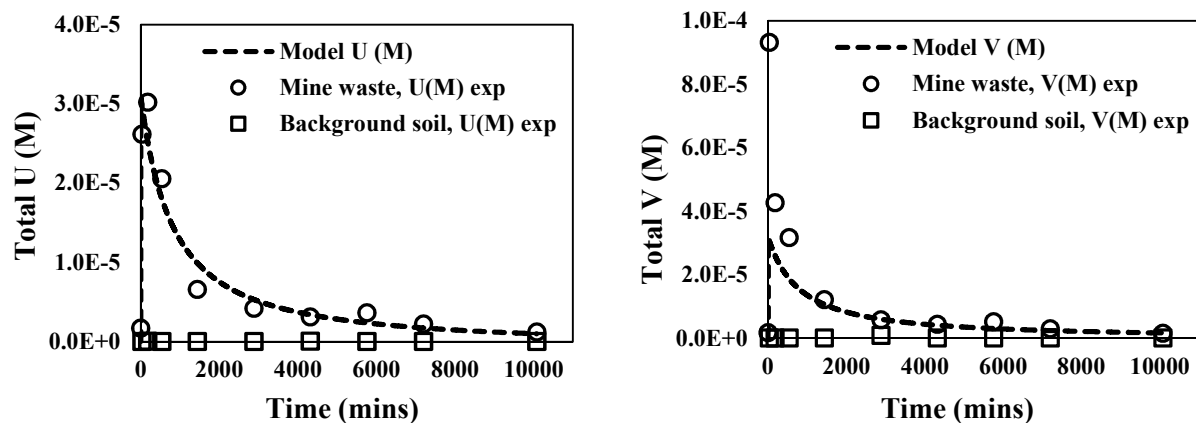


**Figure S4.** Measured and simulated effluent concentrations and reactive transport model (PFLOTRAN) of U and V, from mine waste (circle) and background soil (squares) during continuous flow-through column experiments at pH 7.9 (using 10 mM  $\text{HCO}_3^-$ ), as a function of time. **A)** U concentration versus time; **B)** V concentration versus time. The curve fitting using PFLOTRAN are presented with dashed lines.

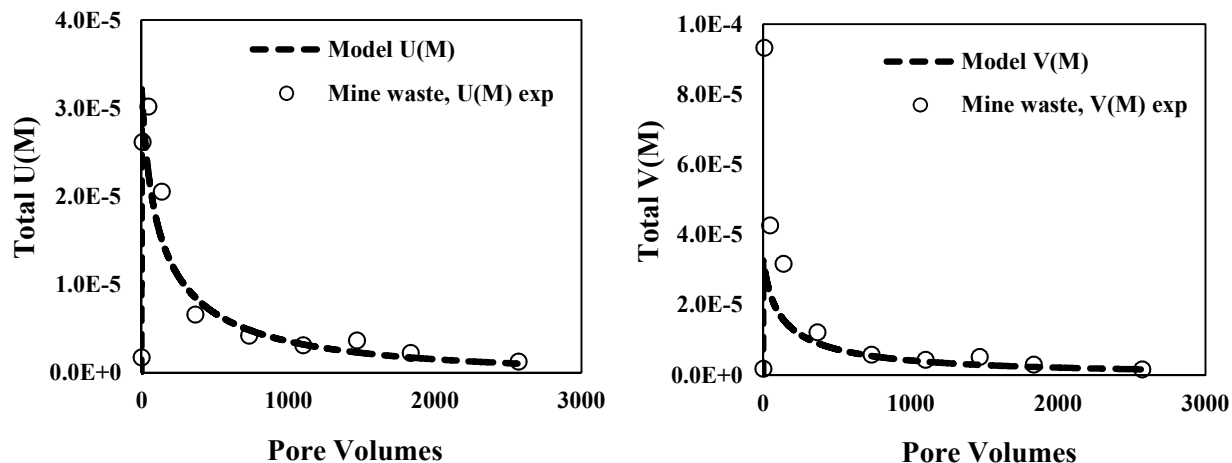


**Figure S5.** Measured and simulated effluent concentrations and reactive transport model (PFLOTRAN) of U and V from mine waste (circle) as a function of pore volumes after considering the effect of grain size during continuous flow-through column experiments at pH 7.9 (using 10 mM  $\text{HCO}_3^-$ ). **A)** U concentrations versus pore volumes **B)** V concentrations versus pore volumes. The curve fitting using PFLOTRAN are presented with dashed lines.

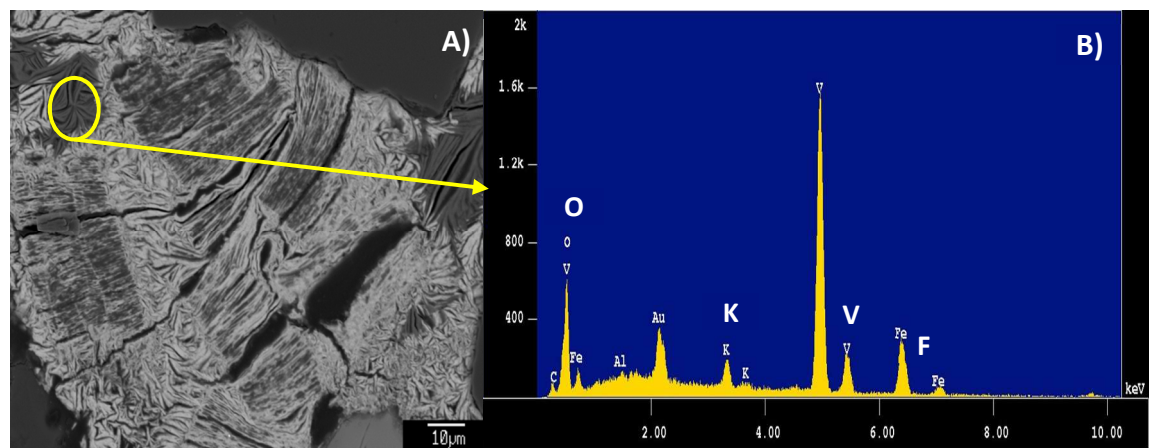


**Figure S6.** Microprobe identification of a V-Fe-K phase in the mine waste samples. **A)** Back Scatter Electron Imaging (BSE) of a V-Fe-K phase. **B)** EDS spectrum of the identified V-Fe-K phase.



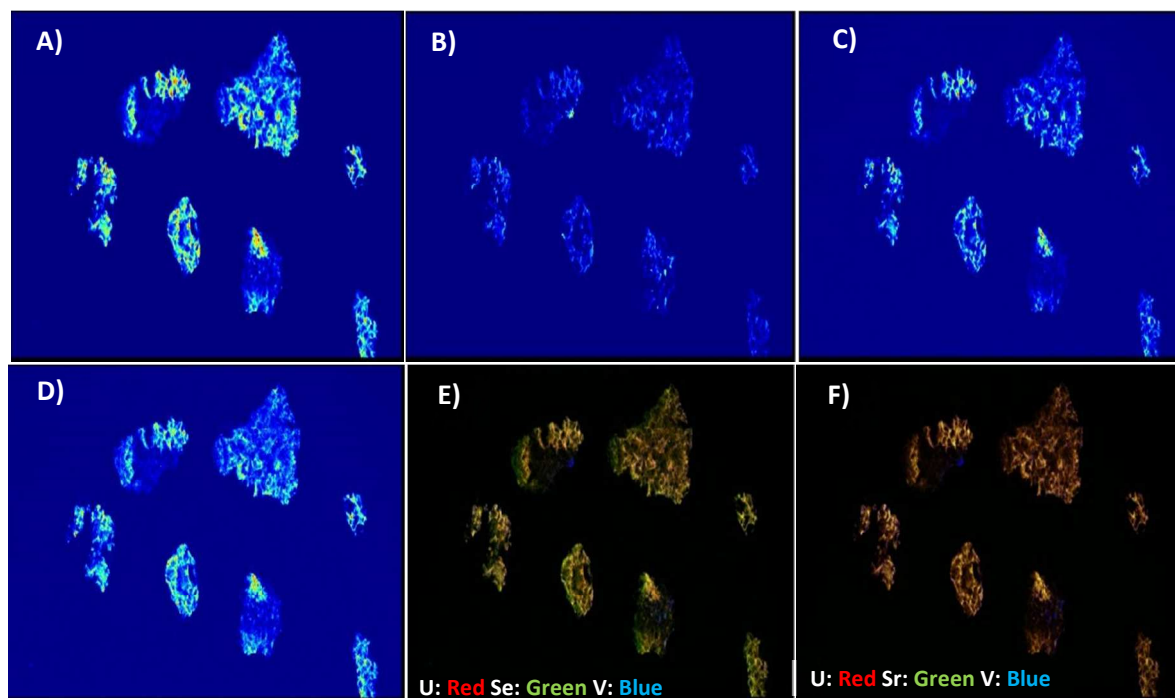


**Figure S7.** Synchrotron Micro- X-ray Fluorescence mapping for mine waste samples identifying the co-occurrence of U with other metals. **A)** Uranium map; **B)** Vanadium map; **C)** Selenium map ; **D)** Strontium map ; **E)** Overlay map of U- red, Se – green and V – blue; **F)** Overlay map of U- red, Sr – green and V – blue. Gradient yellow colors in E and F suggest potential co-occurrence of U and Se, and U and Sr respectively. Similarly cyan gradient colors in E and F suggest co-occurrence of U and V, possibly as a U-V mineral.

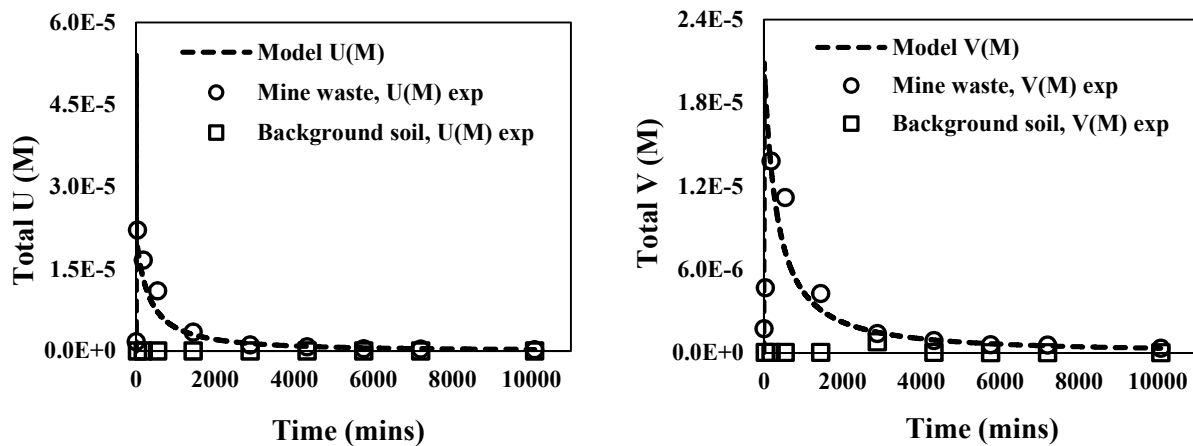


**Figure S8.** Measured and simulated effluent concentrations and reactive transport model (PFLOTRAN) of U and V, from mine waste (circle) and background soil (squares) during continuous flow-through column experiments at pH 3.4 (using 10 mM CH<sub>3</sub>COOH) as a function of time. **A)** U concentration versus time; **B)** V concentration versus time. The curved fitting using PFLOTRAN are presented with solid lines.

## References.

1. Lichtner, P. C., Continuum model for simultaneous chemical reactions and mass transport in hydrothermal systems. *Geochim. Cosmochim. Acta* **1985**, *49* (3), 779-800.
2. Lichtner, P. C., Kinetic rate laws invariant to scaling the mineral formula unit. *Am. J. Sci.* **2016**, *316* (5), 437-469.
3. Lasaga, A. C., Chemical kinetics of water-rock interactions. *J. Geophys. Res. B.* **1984**, *89* (B6), 4009-4025.
4. Brantley, S. L., Kinetics of mineral dissolution. In Kinetics of water-rock interaction, *Springer*: 2008; pp 151-210.
5. Bai, J.; Liu, C.; Ball, W. P., Study of sorption-retarded U(VI) diffusion in Hanford silt/clay material. *Environ. Sci. Technol.* **2009**, *43* (20), 7706-7711.
6. Appelo, C. A. J.; Postma, D., Geochemistry, groundwater and pollution. CRC press: 2004.
7. Blake, J. M.; Avasarala, S.; Artyushkova, K.; Ali, A.-M. S.; Brearley, A. J.; Shuey, C.; Robinson, W. P.; Nez, C.; Bill, S.; Lewis, J., Elevated concentrations of U and co-occurring metals in abandoned mine wastes in a northeastern Arizona Native American community. *Environ. Sci. Technol.* **2015**, *49* (14), 8506-8514.
8. Shock, E. L.; Helgeson, H. C., Calculation of the thermodynamic and transport properties of aqueous species at high pressures and temperatures: Correlation algorithms for ionic species and equation of state predictions to 5 kb and 1000°C. *Geochim. Cosmochim. Acta* **1988**, *52* (8), 2009-2036.
9. Ulrich, K.-U.; Singh, A.; Schofield, E. J.; Bargar, J. R.; Veeramani, H.; Sharp, J. O.; Bernier-Latmani, R.; Giammar, D. E., Dissolution of biogenic and synthetic UO<sub>2</sub> under varied reducing conditions. *Environ. Sci. Technol.* **2008**, *42* (15), 5600-5606.
10. Cox, J.; Wagman, D. D.; Medvedev, V. A., Codata key values for thermodynamics. *Chem/Mats-Sci/E*: **1989**.
11. Pokrovskii, V. A.; Helgeson, H. C., Thermodynamic properties of aqueous species and the solubilities of minerals at high pressures and temperatures; the system Al<sub>2</sub>O<sub>3</sub>-H<sub>2</sub>O-NaCl. *Am. J. Sci.* **1995**, *295* (10), 1255-1342.
12. Baes, C. F.; Mesmer, R. E., Hydrolysis of cations. Wiley: 1976.
13. Johnson, J. W.; Oelkers, E. H.; Helgeson, H. C., SUPCRT92: A software package for calculating the standard molal thermodynamic properties of minerals, gases, aqueous species, and reactions from 1 to 5000 bar and 0 to 1000°C. *Comput. Geosci.* **1992**, *18* (7), 899-947.
14. Wagman, D. D.; Evans, W. H.; Parker, V. B.; Schumm, R. H.; Halow, I. The NBS tables of chemical thermodynamic properties. Selected values for inorganic and C1 and C2 organic substances in SI units; DTIC Document: 1982.
15. Turner, D.; Whitfield, M.; Dickson, A., The equilibrium speciation of dissolved components in freshwater and sea water at 25°C and 1 atm pressure. *Geochim. Cosmochim. Acta* **1981**, *45* (6), 855-881.
16. Mattigod, S. V.; Sposito, G., Chemical modeling of trace metal equilibria in contaminated soil solutions using the computer program *Geochem.* ACS Publications: 1979.
17. Grenthe, I.; Fuger, J.; Konings, R. J.; Lemire, R. J.; Muller, A. B.; Nguyen-Trung, C.; Wanner, H., Chemical thermodynamics of uranium. North-Holland Amsterdam: 1992; Vol. 1.

18. Dong, W.; Brooks, S. C., Determination of the formation constants of ternary complexes of uranyl and carbonate with alkaline earth metals ( $Mg^{2+}$ ,  $Ca^{2+}$ ,  $Sr^{2+}$ , and  $Ba^{2+}$ ) using anion exchange method. *Environ. Sci. Technol.* **2006**, *40* (15), 4689-4695.
19. Bernhard, G.; Geipel, G.; Reich, T.; Brendler, V.; Amayri, S.; Nitsche, H., Uranyl (VI) carbonate complex formation: Validation of the  $Ca_2UO_2(CO_3)_3$  (aq.) species. *Radiochim. Acta* **2001**, *89* (8), 511-518.
20. Israel, Y.; Meites, L.; Bard, A., Encyclopedia of Electrochemistry of the Elements. *Vol. 7* Dekker, New York **1976**, 293.
21. Langmuir, D., Uranium solution-mineral equilibria at low temperatures with applications to sedimentary ore deposits. *Geochim. Cosmochim. Acta* **1978**, *42* (6), 547-569.
22. Sergeeva, E.; Khodakovskiy, I., Physicochemical conditions of formation of native arsenic in hydrothermal deposits. **1969**.
23. Helgeson, H. C., Summary and critique of the thermodynamic properties of rock-forming minerals. *Am. J. Sci.* **1978**, *278*, 1-229.
24. Casas, I.; Bruno, J.; Cera, E.; Finch, R. J.; Ewing, R. C., Characterization and dissolution behavior of a becquerelite from Shinkolobwe, Zaire. *Geochim. Cosmochim. Acta* **1997**, *61* (18), 3879-3884.
25. Robie, R. A.; Hemingway, B. S. Thermodynamic properties of minerals and related substances at 298.15 K and 1 bar ( $10^5$  Pascals) pressure and at higher temperatures; USGPO; For sale by US Geological Survey, Information Services: 1995.
26. Stumm, W.; Morgan, J., Aquatic Chemistry. Interscience, New York: 1970.
27. Meinrath, G.; Kimura, T., Behaviour of U(VI) solids under conditions of natural aquatic systems. *Inorg. Chim. Acta* **1993**, *204* (1), 79-85.
28. Riba, O.; Walker, C.; Ragnarsdottir, K. V., Kinetic studies of synthetic metaschoepite under acidic conditions in batch and flow experiments. *Environ. Sci. Technol.* **2005**, *39* (20), 7915-7920.
29. Bond, D. L.; Davis, J. A.; Zachara, J. M., Uranium (VI) release from contaminated vadose zone sediments: Estimation of potential contributions from dissolution and desorption. *Developments in Earth and Environmental Sciences* **2007**, *7*, 375-416.